First-principles calculations of solid and liquid aluminum optical absorption spectra near the melting curve: Ambient and high-pressure results

Tadashi Ogitsu, Lorin X. Benedict, Eric Schwegler, and Erik W. Draeger
Lawrence Livermore National Laboratory, Livermore, California 94550, USA

David Prendergast
Lawrence Berkeley National Laboratory, Berkeley, California 94720, USA

We present *ab initio* calculations of the linear optical conductivity of heated Al at ambient pressure and at the conditions relevant for shock melting ($P \sim 125$ GPa, $T \sim 5000$ K). It is shown that the visible and near-UV optical spectrum is very sensitive to the phase (fcc solid versus liquid) of Al for both $P = 0$ and 125 GPa. The ambient-P results confirm an earlier prediction and the results of a recent experiment while the high-(P, T) results allow us to conclude that *in situ* measurements of optical constants should be able to diagnose the shock melting of Al.

I. INTRODUCTION

The study of the optical properties of heated solids has been of particular interest over the last 15 years, largely because of the possibility of using optical measurements to detect changes induced in a material by intense laser excitation.[1–3] In these studies, the material is first heated by an ultrashort pulsed high-intensity laser, and after some time delay, the optical spectrum is probed by a (possibly broadband) light source. Upon application of the pump pulse, the electrons are heated first, and after some time they exchange energy with the cooler ions. If the fluence of the pump laser is high enough, it is possible to induce a phase change in which the crystalline lattice of ions is eventually destabilized and the material is left in a disordered amorphous or liquid state. At very short times after the pump, before the ions have moved appreciably, changes in an optical spectrum can be observed which are a result of the heated electron distribution.[2,4] For longer delay times, it has been shown that the linear optical absorption spectrum can exhibit dramatic changes resulting from the ion disorder.[2,5] These changes are particularly pronounced in the laser excitation of semiconductors such as Si and GaAs, since the amorphous forms of these materials are metallic, and the low-frequency optical conductivity of a metallic system is qualitatively different from that of a semiconductor.

Optical properties should be different for ordered and disordered phases of metals as well, though the differences may be less pronounced since both phases are metallic. An interesting test case in this regard is aluminum. The electronic single-particle bands of fcc solid Al are well described by the nearly free-electron model.[6,7] As such, it is not unreasonable to suspect that the optical spectra of both the fcc solid and the relatively closed-packed liquid may be quite similar. Measurements by Krishnan and Nordine[8] support this view; they measured the absorption spectrum in liquid Al at $T = 1550$ K to be very similar to that of the heated solid. As they noted however, this result was somewhat surprising: The absorption spectrum of the cold solid possesses a strong peak at $\hbar\omega \sim 1.5$ eV, known to result from transitions between nearly parallel electronic bands.[7,9] In the liquid, one might have expected these detailed band featured to be washed out, giving rise to a Drude-type spectrum with no peaks at nonzero frequencies.[10] More recent measurements by Kandyla *et al.*[11] indicate that the liquid and the heated solid do indeed have notably different spectra. These researchers found the spectrum of liquid Al to be devoid of the peaks seen for the fcc phase, in contradiction to the Krishnan and Nordine result. In addition, a recent calculation[12] of the T-dependent optical absorption spectrum of Al using classical molecular dynamics (MD) for the ions and an empirical pseudopotential treatment for the electronic states predicts a Drude-type optical spectrum for the liquid while reproducing the measured T dependence of the spectrum of the solid.[13]

All of the aforementioned studies address ambient pressure. Another reason for the interest in the optical response of heated materials is the possibility of using optical measurements as an *in situ* diagnostic for phase change in a shock experiment. Considering the case of Al, if the absorption spectra of the solid and the liquid were quite different at the conditions of shock melting, the precise point along the compression path corresponding to the phase transition could be identified. Though the absorption spectrum of Al at elevated pressures has been investigated both experimentally and theoretically,[14–16] the highest pressures were well below the shock-melting pressure (~ 125 GPa) and the studies were confined to room temperature.

In this work, we present *ab initio* calculations of the linear optical absorption spectrum of heated Al at ambient pressure and at the pressure and temperature corresponding to what is believed to be shock-melting conditions ($P \sim 125$ GPa, $T \sim 5000$ K). In both cases, we compute the fcc solid and liquid spectra and show that even for identical conditions of density and temperature, solid and liquid spectra show marked differences. We therefore conclude that the measurement of optical spectra in the visible and near UV during a shock experiment would enable the determination of the onset of shock melting. This could be an attractive way of observing phase change in a dynamic high-P experiment since the technical challenges of fielding a time-resolved *in*

situ x-ray diffraction diagnostic are still formidable.[17]

II. COMPUTATION OF $\sigma_1(\omega)$

In order to compute the spectrum of heated Al, we must average over ionic configurations corresponding to the appropriate (P, T) conditions. We produce these configurations with *ab initio* Born-Oppenheimer MD (BOMD) based on density-functional theory.[18] The question of the size of the periodic MD cell is an important one. The study of Ref. 12 using empirical methods showed that fewer than ten uncorrelated configurations of a 32-atom cell were needed to converge the optical spectrum of the heated fcc solid; the liquid was found to require still fewer configurations of the same size. Our studies using *ab initio* electronic structure techniques reveal the same dependences. In this study, we have used both a 32-atom cell and a 108-atom cell and have assessed the effect of size on the optical conductivity. We did not find a qualitative difference in the optical conductivities calculated with the 32-atom cell and with the 108-atom cell. However, the fluctuations in the optical spectra from snapshot to snapshot were slightly larger with the 32-atom cell indicating a small yet visible size effect with this cell. Therefore, in this paper, we only present the results obtained with the 108-atom cell, although the data produced with the 32-atom cell leads to the same conclusions.

Ab initio BOMD simulations were performed with the QBOX code.[19] The Al pseudopotential was chosen to be of the Troulier-Martins form[20] with s, p-nonlocal and d-local channels. We used two (folded) Chadi-Cohen special k points[21] appropriate for fcc for the sampling of the electronic states and a plane-wave energy cutoff of 20 Ry in the self-consistent field calculations to determine the electronic charge density for each ionic configuration. We examined the convergence of the ionic forces as a function of k-point sampling, and found that the Chadi-Cohen two special k points[21] provides the same level of convergence as an $8 \times 8 \times 8$ Monkhorst-Pack grid, while a single off-Γ sampling such as the Baldereschi point[22] exhibits larger discrepancy from the $8 \times 8 \times 8$ Monkhorst-Pack grid, although it shows significant improvement over Γ-point sampling. A time step of 1.5 fs and a velocity-scaling thermostat with a response time of 100 fs was used when performing the MD for the ions. Snapshots with which we computed the optical response were taken 1.5 ps apart, which we deemed to be sufficient for generating uncorrelated ionic configurations. We left the thermostat on during the computation of the ionic snapshots; detailed comparison of the radial distribution function, $g(r)$, and diffusion constant, determined with and without the thermostat showed a negligible effect on the ion dynamics. In all of these simulations, the electronic temperature was set equal to the ionic temperature.

For each snapshot, the real part of the long-wavelength frequency-dependent optical conductivity, $\sigma_1(\omega)$, was calculated with the random-phase approximation (RPA) expression for σ derived from a Kubo-type response formula,[23]

$$\sigma_1(\omega) = \lim_{\mathbf{q} \to 0} \frac{2e^2 \omega}{\Omega q^2} \sum_{c,v,\mathbf{k}} |\langle v, \mathbf{k} | e^{-i\mathbf{q} \cdot \mathbf{r}} | c, \mathbf{k} + \mathbf{q} \rangle|^2$$
$$\delta[E_c(\mathbf{k} + \mathbf{q}) - E_v(\mathbf{k}) - \hbar\omega][f_v(\mathbf{k}) - f_c(\mathbf{k} + \mathbf{q})]. \tag{1}$$

Here, v and c denote conduction and valence bands, E are the quasiparticle band energies for the electrons, f are their Fermi-Dirac thermal occupation numbers, $\mathbf{k}$ and $\mathbf{q}$ are crystal momenta, and Ω is the system volume. Note that this approach involves summing over transitions between *single*-electron states, and therefore neglects excitons and other multiparticle excitations. Electronic states were computed using the local-density approximation (LDA) with the PWSCF code[24] with the Perdew-Zunger parameterization of the exchange-correlation potential.[25] The pseudopotential used to calculate the optical conductivity was exactly the same as the one used to perform the BOMD. Also, since we use LDA electronic states for $E(\mathbf{k})$ and $|\mathbf{k}\rangle$, we neglect quasiparticle self-energy corrections. This LDA-RPA treatment is known to work well for predicting the linear optical response of Al at ambient pressure and low temperatures[26] since metallic screening suppresses self-energy (and excitonic) effects. We expect the treatment to work equally well for the higher temperatures we consider here. Indeed, our highest temperatures are still well below the Fermi temperature, and even if they had been quite a bit higher, it is likely that LDA/generalized gradient approximation would have worked even better.[27]

In order to render accurately the prominent peak in the absorption spectrum of the fcc solid phase, it is necessary to use a very large number of k points in the sum of Eq. (1).[12,26] We used a $32 \times 32 \times 32$ k-point mesh for our solid snapshot calculations at 300 K while for the higher temperatures, a $24 \times 24 \times 24$ k-point mesh was sufficient to obtain a converged spectrum. In a related point, we represented the δ function of Eq. (1) as a Gaussian with $\sigma = 0.1$ eV (full width at half maximum of 0.2355 eV).

To reduce the computational effort, we employed the optimal basis set approach to interpolating the LDA electronic states and corresponding matrix elements throughout the first Brillouin zone.[28] Our recent implementation of this approach accurately reproduces the electronic states and energies for large supercells at any k point, based only on explicit LDA calculations at the zone center ($\mathbf{k} = 0$). In this formalism the electronic Hamiltonian matrix elements are polynomials in $\mathbf{k}$. This is advantageous for explicit evaluation of the limit in Eq. (1) using the identity

$$\lim_{\mathbf{q} \to 0} [E_c(\mathbf{k} + \mathbf{q}) - E_v(\mathbf{k})] \frac{\langle v\mathbf{k} | e^{-i\mathbf{q} \cdot r} | c\mathbf{k} + \mathbf{q} \rangle}{q} = \langle u_{v\mathbf{k}} | \frac{dH(\mathbf{k})}{d\mathbf{k}} | u_{c\mathbf{k}} \rangle, \tag{2}$$

where $|u_{n\mathbf{k}}\rangle = e^{-i\mathbf{k} \cdot \mathbf{r}} |n\mathbf{k}\rangle$ are the periodic components of the Bloch functions. The derivative of the Hamiltonian can be evaluated explicitly at a given point without resorting to numerical differentiation using finite $\mathbf{q}$. We have confirmed that this $\mathbf{k}$-space interpolation scheme produces a band structure and an optical spectrum which are essentially identical to those of the standard scheme. With supercell calculations at

finite temperature, we computed the band dispersions for a few select k vectors in the first Brillouin zone using both schemes; comparisons between the two showed excellent agreement (the mean-square deviation was negligibly small on the energy scale of interest).

We note that to estimate $\sigma_1(\omega)$ at a small ω, one may use a Drude approximation to represent the intraband transitions, containing a phenomenological broadening parameter and an accurate estimate of the plasma frequency.[29] We do not use this approach here since at high temperature, the elastic electron-ion scattering arising from the thermally disordered lattice (already included in our supercell calculations) is expected to dominate the contribution to $\sigma_1(\omega)$ in the Drude regime.

Finally, in performing calculations on Al at different temperatures and pressures, we must appeal to an existing equation of state (EOS) for Al to determine the volume per atom, V, for each (P,T). A first-principles calculation of the finite-temperature EOS of Al has been published in the literature.[30] In this work, since our focus is to investigate the optical spectrum of Al under pressure and at high temperature, we use the best available experimental and phenomenological information regarding Al EOS in the literature instead. For the ambient-pressure calculations, we extract V as a function of T from the measured equilibrium density and thermal expansion coefficient.[31] For the liquid at ambient pressure, we use the measured T-dependent liquid density of Ref. 32. These same choices were made in an earlier theoretical study.[12] For the simulations addressing the conditions of shock melting, we use the theoretical multiphase EOS for Al developed at Los Alamos National Laboratory.[33] This EOS was developed using a combination of experimental results and *ab initio* calculations and it was designed to reproduce both the measured melt curve and the pressure-volume relation along the principal shock Hugoniot. We note that this EOS produces a $V(P=0,T)$ in excellent agreement with the aforementioned ambient-pressure data as well. With this EOS we compute the (P,T) point where shock melting is predicted to occur: $P=125$ GPa and $T=5000$ K. Then we determine V corresponding to these conditions for both the solid and the liquid phase.

III. RESULTS AND DISCUSSION

Figure 1 shows our computed optical conductivity of heated Al for $P=0$ ($T=300,550,750,950$ K), and $P=125$ GPa ($T=5000$ K). For the $P=0$ cases, the volume per atom was taken from experiment,[31,32] as we mentioned above; for the $P=125$ (shock melting) case, the volume per atom was taken to be 9.5 Å³/atom, as determined by the LANL Al EOS.[33] Note that while the solid and liquid volumes at the shock-melt point are sure to be different (they are predicted to be different by about 3% in the EOS we used[33]), we chose to use the *same* volume per atom for the solid and liquid calculations at $P=125$ GPa and $T=5000$ K. This volume was chosen to be between the predicted solidus and liquidus volumes at the point of shock melting as calculated by the LANL EOS. In this way, we look *only at the effect of disordering* in the shock-melt case.
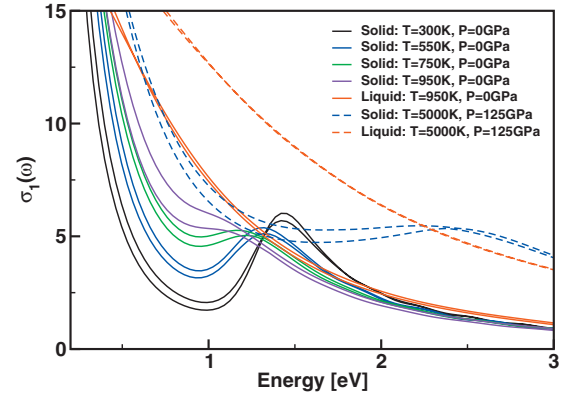

FIG. 1. (Color) The optical conductivity, $\sigma_1(\omega)$, of Al at various (P,T) conditions. For each (P,T) point, maximum and minimum values for σ_1 were taken from ten ionic configurations separated from each other by $\delta t = 1.5$ ps. With the liquid at ($P=125$ GPa, $T=5000$ K), the variation in $\sigma_1(\omega)$ between different ionic configurations is negligibly small, therefore the lines corresponding to the minimum and the maximum practically coincide.

Each spectrum consists of two lines corresponding to the minimum and the maximum values of $\sigma_1(\omega)$ taken from approximately ten uncorrelated ionic configurations (see Fig. 1). We see that the liquid spectra could have been computed with a single ionic configuration (and perhaps with fewer k points). Nevertheless, our use of very conservative values for these parameters ensures that any features present in the LDA-RPA spectra of hot Al would have been resolved since these values are required to converge the spectrum of the $T=300$ K fcc solid.[12]

For $P=0$, we see that the spectrum of the solid evolves with temperature in a manner equivalent to that shown in the experimental work of Ref. 13 and the earlier semiempirical theoretical study:[12] The peak at ~1.5 eV broadens while moving to slightly lower energy as T is increased.[34] In addition, the dip at ~1 eV fills in, leaving only a shoulder in the hot solid in the neighborhood of melting ($T_{melt}=938$ K). In agreement with Ref. 12, the liquid spectrum shows no such shoulder. Thus, hot fcc and liquid Al *at the same temperature* show a markedly different linear optical spectrum. This conclusion is in contrast to the early experimental work of Krishnan and Nordine[8] but is in agreement with the more recent experimental study of Kandyla *et al.*[11] We stress that while our results are very similar to those of Ref. 12, our use of a self-consistent electronic structure scheme lends additional credence to our conclusions, since the rearrangement of electronic charge due to the noncrystalline ionic positions could have altered the electron-ion potential significantly from the superposition of atom-centered potentials assumed in Ref. 12. In addition, the nearly free-electron character exhibited in aluminum at ambient pressures, required for the empirical pseudopotential treatment to produce transferable results for disordered aluminum, is expected to diminish at the higher pressures we now discuss.

For the shock-melt conditions, the peak in the solid is centered at an energy above 2 eV, consistent with lower-T calculations and measurements at elevated pressures.[14,15] Of note is the fact that our predicted difference between solid
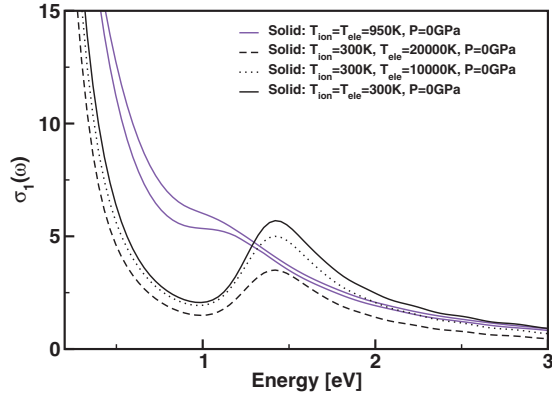
FIG. 2. (Color) The optical conductivity, $\sigma_1(\omega)$, of fcc Al at $T=950$ K (purple lines) is compared to the those at $T_{ion}=300$ K with elevated electron temperatures, $T_{ele}=10\,000$ K and $T_{ele}=20\,000$ K, to demonstrate that the smearing of the interband transition peak due to an elevated electron temperature is different from that due to thermal lattice disorder. The $\sigma_1(\omega)$ for $T_{ion}=T_{ele}=300$ K is also plotted as a reference. The different results for $T_{ion}=300$ K were calculated from the same ionic configuration. The small configuration dependence, seen in Fig. 1, would not substantively affect these results.

and liquid spectra at the point of melting on the principal Hugoniot is even more pronounced than it is at ambient pressures. Again, the liquid spectrum is featureless and Drude-type, and the solid spectrum *at the same density and temperature* has a broadened but still prominent peak. This allows us to suggest that the *in situ* measurement of optical properties during the course of a shock experiment performed on Al may be able to diagnose melting.

Returning again to ambient pressures, we note that changes to the optical spectrum arising from elevated electron temperature are distinctly different from those arising from elevated ion temperature: Since the parallel bands responsible for the interband transition peak at around 1.5 eV span a wide energy range (see, for example, Refs. 7, 9, and 16), raising the electron temperature up to even 20 000 K with the lattice temperature at 300 K does not change the peak position, although the peak height is somewhat suppressed (see Fig. 2). This indicates that, as far as Al is concerned, $\sigma_1(\omega)$ is a good measure of *lattice* disorder and therefore *ion temperature*, even in the case of laser-heated targets where $T_{electron}$ could be significantly higher than T_{ion} for some time.[35]

Our calculations addressing the shock-melt case assume that the system is in thermal equilibrium on both sides of the transition. In addition, the fact that we have appealed to an EOS implies that the transition is not overdriven due to ki-

netics. These assumptions may not be justified in reality since the material may remain in a superheated solid phase for some time. Even in this case, we argue that since our results show that solid and liquid possess qualitatively distinct spectra due to the different nature of the ion disorder in both phases, time-resolved measurement of the optical reflectivity in the 1–3 eV photon energy range should facilitate the determination of the shock-induced phase transformation time.[36]

IV. CONCLUSIONS

We have computed the linear optical absorption spectrum of heated Al in the visible and near UV using *ab initio* electronic-structure methods. Atomic positions were determined by performing *ab initio* molecular dynamics for a periodically repeated cell of 108 atoms with two special k points. For each MD snapshot used, the spectrum was calculated with the RPA with single-electron states determined by self-consistent LDA calculations on a dense k-point grid. Two pressures were considered: $P=0$ and $P=125$ GPa. In the ambient-pressure case, we computed the spectrum for temperatures ranging from 300 to 950 K. For 950 K, both solid and liquid were considered. We found the spectrum for photon energies from 0.5–2 eV to be notably different for hot solid and liquid Al, in agreement with earlier semiempirical calculations[12] and a recent experiment,[11] but in disagreement with earlier experimental results.[8] We studied the $P=125$ GPa, $T=5000$ K case to address shock melting. Here we found an even more notable difference between hot solid and liquid spectra, though the spectral features are pushed to higher photon energies. The pronounced difference between the optical properties of Al just above and below melt in the neighborhood of shock melting allows us to suggest that *in situ* time-resolved measurements of the optical spectrum could provide a reliable diagnostic for the precise onset of melting. Other materials may be amenable to this analysis as well; we expect the sensitivity of linear optical spectra to phase in the neighborhood of melting to be strongly material dependent and phase dependent.

[1] P. Celliers, A. Ng, G. Xu, and A. Forsman, Phys. Rev. Lett. **68**, 2305 (1992); A. Ng, P. Celliers, G. Xu, and A. Forsman, Phys. Rev. E **52**, 4299 (1995).

[2] L. Huang, J. P. Callan, E. N. Glezer, and E. Mazur, Phys. Rev. Lett. **80**, 185 (1998); J. P. Callan, A. M. T. Kim, L. Huang, and E. Mazur, Chem. Phys. **251**, 167 (2000).

[3] Y. Ping, D. Hanson, I. Koslow, T. Ogitsu, D. Prendergast, E. Schwegler, G. Collins, and A. Ng, Phys. Rev. Lett. **96**, 255003

(2006).

[4] L. X. Benedict, Phys. Rev. B **63**, 075202 (2001).

[5] J. S. Graves and R. E. Allen, Phys. Rev. B **58**, 13627 (1998).

[6] W. A. Harrison, Phys. Rev. **118**, 1182 (1960); **118**, 1190 (1960).

[7] N. W. Ashcroft, Philos. Mag. **8**, 2055 (1963); N. W. Ashcroft and K. Sturm, Phys. Rev. B **3**, 1898 (1971).

[8] S. Krishnan and P. C. Nordine, Phys. Rev. B **47**, 11780 (1993); **48**, 4130 (1993).

[9] J. P. Walter, C. Y. Fong, and M. L. Cohen, Solid State Commun. **12**, 303 (1973).

[10] J. Miller, Philos. Mag. **20**, 1115 (1969).

[11] M. Kandyla, T. Shih, and E. Mazur, Phys. Rev. B **75**, 214107 (2007).

[12] L. X. Benedict, J. E. Klepeis, and F. H. Streitz, Phys. Rev. B **71**, 064103 (2005).

[13] A. G. Mathewson and H. P. Meyers, J. Phys. F: Met. Phys. **2**, 403 (1972).

[14] H. Tups and K. Syassen, J. Phys. F: Met. Phys. **14**, 2753 (1984).

[15] R. G. Dandrea and N. W. Ashcroft, Phys. Rev. B **32**, 6936 (1985).

[16] M. Alouani and M. A. Khan, J. Phys. (France) **47**, 453 (1986).

[17] P. A. Rigg and Y. M. Gupta, Phys. Rev. B **63**, 094112 (2001); J. A. Hawreliak, D. H. Kalantar, J. S. Stölken, B. A. Remington, H. E. Lorenzana, and J. S. Wark, *ibid.* **78**, 220101(R) (2008).

[18] P. Hohenberg and W. Kohn, Phys. Rev. **136**, B864 (1964); W. Kohn and L. J. Sham, *ibid.* **140**, A1133 (1965).

[19] QBOX first-principles molecular dynamics code, LLNL version 1.47.0, written by F. Gygi (http://eslab.ucdavis.edu) and further developed by E. W. Draeger. QBOX is a C++/MPI scalable parallel first-principles MD implementation based on the plane-wave pseudopotential formalism.

[20] N. Troullier and J. L. Martins, Phys. Rev. B **43**, 1993 (1991).

[21] D. J. Chadi and M. L. Cohen, Phys. Rev. B **8**, 5747 (1973).

[22] A. Baldereschi, Phys. Rev. B **7**, 5212 (1973).

[23] H. Ehrenreich and M. H. Cohen, Phys. Rev. **115**, 786 (1959).

[24] QUANTUM-ESPRESSO is a community project for high-quality quantum-simulation software based on density-functional theory and coordinated by Paolo Giannozi, see http://www.quantum-espresso.org and http://www.pwscf.org

[25] J. P. Perdew and A. Zunger, Phys. Rev. B **23**, 5048 (1981).

[26] L. X. Benedict, C. D. Spataru, and S. G. Louie, Phys. Rev. B **66**, 085116 (2002).

[27] S. V. Faleev, M. van Schilfgaarde, T. Kotani, F. Leonard, and M. P. Desjarlais, Phys. Rev. B **74**, 033101 (2006).

[28] E. L. Shirley, Phys. Rev. B **54**, 16464 (1996).

[29] C. Ambrosch-Draxl and J. O. Sofo, Comput. Phys. Commun. **175**, 1 (2006).

[30] L. Vočadlo and D. Alfé, Phys. Rev. B **65**, 214105 (2002).

[31] Y. S. Touloukian, R. K. Kirby, R. E. Taylor, and T. Y. R. Lee, *Thermophysical Properties of Matter*, 2n ed. edited by Y. S. Touloukian, R. K. Kirby, R. E. Taylor, and P. D. Desai, Vol. 12, (IFI/Plenum, New York, NY, 1977), p. 2.

[32] E. I. Gol'tsova, High Temp **3**, 438 (1965).; [Teplofiz. Vis. Temp. **3**, 438 (1965)].

[33] E. D. Chisolm, S. D. Crockett, and D. C. Wallace, Phys. Rev. B **68**, 104103 (2003).

[34] At lower temperatures for the $P=0$ case, the width of our peak in $\sigma_1(\omega)$ is notably smaller than that presented in the experimental results of Ref. 13. This can also be seen in the theory-experiment comparison shown in Ref. 12. Quasiharmonic lattice-dynamics calculations for Al show that this discrepancy is primarily due to the complete neglect of zero-point motion in the theoretical work, in which the ions are treated *classically* in the MD. This point was not made in Ref. 12. At the higher temperatures of greater interest here, the zero-point motion effect is small compared to the thermally induced disordering of the ion positions treated appropriately in the MD.

[35] This analysis does not take into account the increase in the peak width or changes to the peak position coming from quasiparticle self-energy effects. However, the results of Ref. 26 suggest that these would be relatively minor for $T=20\,000$ K and below.

[36] D. Orlikowski, J. H. Nguyen, J. R. Patterson, R. Minich, L. P. Martin, and N. C. Holmes, in *Shock Compression of Condensed Matter-2007*, edited by M. Elert M. D. Furnish, and R. Chau, (American Institute of Physics, New York, 2007), p. 1186.